

Marquette University

e-Publications@Marquette

---

Electrical and Computer Engineering Faculty  
Research and Publications

Electrical and Computer Engineering,  
Department of

---

11-2018

## Impacts of Operators' Behavior on Reliability of Power Grids During Cascading Failures

Zhuoyao Wang

Mahshid Rahnamay-Naeini

Joana M. Abreu

Rezoan A. Shuvro

Pankaz Das

*See next page for additional authors*

Follow this and additional works at: [https://epublications.marquette.edu/electric\\_fac](https://epublications.marquette.edu/electric_fac)



Part of the [Computer Engineering Commons](#), and the [Electrical and Computer Engineering Commons](#)

---

---

**Authors**

Zhuoyao Wang, Mahshid Rahnamay-Naeini, Joana M. Abreu, Rezoan A. Shuvro, Pankaz Das, Andrea Mammoli, Nasir Ghani, and Majeed M. Hayat

---

Marquette University

**e-Publications@Marquette**

***Electrical and Computer Engineering Faculty Research and Publications/College of Engineering***

***This paper is NOT THE PUBLISHED VERSION.***

Access the published version via the link in the citation below.

*IEEE Transactions on Power Systems*, Vol. 33, No. 6 (November 2018): 6013-6024. [DOI](#). This article is © Institute of Electrical and Electronics Engineers and permission has been granted for this version to appear in [e-Publications@Marquette](#). Institute of Electrical and Electronics Engineers does not grant permission for this article to be further copied/distributed or hosted elsewhere without the express permission from Institute of Electrical and Electronics Engineers.

# Impacts of Operators' Behavior on Reliability of Power Grids During Cascading Failures

Zhuoyao Wang

Department of Electrical and Computer Engineering and Center for High Technology Materials, University of New Mexico, Albuquerque, NM

Mahshid Rahnamay-Naeini

Electrical Engineering Department, University of South Florida, Tampa, F

Joana M. Abreu

Fraunhofer Center for Sustainable Energy Systems, Boston, MA

Rezoan A. Shuvro

Department of Electrical and Computer Engineering and Center for High Technology Materials, University of New Mexico, Albuquerque, NM

Pankaz Das

Department of Electrical and Computer Engineering and Center for High Technology Materials, University of New Mexico, Albuquerque, NM

Andrea A. Mammoli

Mechanical Engineering Department, University of New Mexico, Albuquerque, NM

**Nasir Ghani**

Electrical Engineering Department, University of South Florida, Tampa, FL

**Majeed M. Hayat**

Department of Electrical and Computer Engineering and Center for High Technology Materials, University of New Mexico, Albuquerque, NM

## **Abstract:**

Human operators play a key role in the reliable operation of critical infrastructures. However, human operators may take actions that are far from optimum. This can be due to various factors affecting the operators' performance in time-sensitive and critical situations such as reacting to contingencies with significant monetary and social impacts. In this paper, an analytic framework is proposed based on Markov chains for modeling the dynamics of cascading failures in power grids. The model captures the effects of operators' behavior quantified by the probability of human error under various circumstances. In particular, the observations from historical data and information obtained from interviews with power-system operators are utilized to develop the model as well as identify its parameters. In light of the proposed model, the noncritical regions of power-system's operating characteristics with human-factor considerations are characterized under which the probability of large cascading failures is minimized.

## **SECTION I. Introduction**

Critical infrastructures, such as power grids, are being increasingly equipped with advanced technologies and mechanisms including monitoring, automated control, intelligence and computational resources to enhance their reliability. However, human operators remain to be a key element in the reliable operation of such systems with often critical decisions to make and actions to take. In particular, the historical data of various infrastructure contingencies, such as the 2003 Northeast [1] and the 2011 Southwest [2] blackouts, show a clear track of operators' decisions and actions that significantly contributed, both positively and negatively, in the events. Specifically, critical and stressful situations, such as reacting to contingencies with significant monetary and social impacts, can affect human performance and increase the likelihood of human errors in decisions and actions. As discussed in [3], [4], it is not easy to model the human component in vulnerability analysis of critical infrastructures; however, efforts with various focuses on different infrastructures and contingency scenarios have emerged to address the critical need for understanding the role of human factors in the reliability of power-grid operations [5]–[9].

It is well known that large-scale blackouts in power grids are typically caused by cascading failures. The risk and high impact of cascading failures have attracted the attention of many researchers in the past and they have exerted considerable efforts in understanding and characterizing this phenomenon [10]–[18]. Nonetheless, the role of human factors in cascading failures has not been modeled and investigated analytically in the existing studies to the best of our knowledge.

Several factors can shape the performance of human operators in making critical decisions with potentially detrimental or beneficial effects on the physical system. Examples of such factors include the psychological state of the operators at the time of the event, level of stress, fatigue, level of

experience, the amount of time to respond to a situation, knowledge and awareness about the situation, etc. Many of these factors are tied to the state of the physical system, and as the physical system evolves in time so do these factors and consequently the performance of human operators. At the same time, the human operators' performance can directly affect the state of the physical system through decisions and actions. As such, there is a coupling between the dynamics of the physical system and the human factors, which makes the analysis of cascading failures particularly challenging.

In this paper, we capture the coupling between the human factors and the power grid in an analytic framework. In particular, the proposed framework consists of two key components: (i) a Markov-chain model for the dynamics of cascading failures in the power grid, and (ii) a human reliability assessment model to characterize the probability of human error (by utilizing the Standardized Plant Analysis Risk-Human (SPAR-H) Reliability Analysis Method [19]) to investigate the effects of human factors on the progression of cascading failures in the power grid. These components are integrated together through various model parameters and state variables to capture the coupling between cascading dynamics and the human factors.

The proposed framework enables us to investigate the effects of human behavior on cascading phenomenon in power grids. We specifically characterize the probabilities of progression of cascading failures with various sizes of blackouts under various disturbance scenarios. We further provide the non-critical region of power-system operating characteristics (including loading level, load-shedding constraints and line-tripping threshold), which makes the power grid behave less vulnerable to cascading failures (i.e., the blackout size is distributed exponentially rather than one with a power-law tail), while considering the effects of human behavior.

## SECTION II. Related Work

In this section we review three categories of work related to this paper. The first category is the work on the analysis of human reliability and performance. The second category of related work is on modeling the impact of human factors on critical infrastructures. The third and last category is on the modeling of cascading failures in power grids.

Human error can affect the system's performance just like any other technical flaw [20]. Human reliability analysis (HRA) is a technique designed to determine the critical aspects and the errors that can affect human decision making. HRA encapsulates the following steps: description of tasks in a chain of events, dependence among tasks, procedures and processes, situation awareness and cognitive conditions of the decision maker [5]. The SPAR-H is a simplified approach to human-error quantification that accounts for individual perception processing and response to events in complex environments [21]. The method relies on the multiplicative effect of performance shaping factors (PSFs), which are variables that describe the situation or the psychological condition of the human operators. Each factor contains levels of severity. The outcome of the SPAR-H methodology is the calculation of a total Human Error Probability (HEP) for every diagnosis or action in the event tree [22]. Abreu *et al.* [7] modeled the HEP in various failure scenarios by interviewing power-system operators with different levels of expertise. In [8], Panteli and Kirschen investigated how insufficient operators' situation awareness affect cascading failures in power systems; then a generic procedure was presented for achieving sufficient situation awareness.

As for the second category of the related work, we review the existing models that investigated the impact of human factors in critical infrastructures. In [13], Anghel *et al.* presented a stochastic model to provide a comprehensive representation of the complex behavior of both the grid dynamics under random perturbations and the operator's response to the contingency events. This model described the utility response to various disturbances in an attempt to include a description of the human response to contingency events. Numerical results were presented to cast the optimization of operators' response into the choice of the optimal strategy for mitigating the impact of random component failure events and, possibly, for controlling blackouts. In [6], Lawton and Gauthier developed an approach to integrate human performance modeling into a large scale system-of-systems (SoS) simulation toolset. The SoS-scale analysis on human performance was presented and the utility of the toolset was illustrated by an example problem. In [9], Bessani *et al.* introduced a stochastic model to enable the incorporation of human operators' performance in a sequential Monte-Carlo simulation that integrates the response time in reliability of power systems. Their results showed that the response time of the operators affects the reliability that are related to the durations of the failure, indicating that a fast decision directly contributes to the system performance. In [23], Moura *et al.* introduced the multi-attribute technological accidents dataset (MATA-D) containing detailed investigation reports from the past major accidents and used it to address the manifestation of human errors.

As for the third category of related work, we shall discuss the probabilistic models and statistical analysis of cascading failures in power grids. In [24], Carreras *et al.* asserted that the frequency distribution of the blackout sizes does not decrease exponentially with the size of the blackout, but rather has a power-law tail. Such important observation was obtained from the analysis of a 15-year time series of blackouts in the North American electric power transmission system. A simplified power-transmission-system model was then presented to examine the criticality of cascading failures in the transmission system. The model considered the DC power flow approximation and standard linear programming optimization of the generation dispatch. In [25], Kirschen *et al.* proposed a technique to calculate a probabilistic indicator of the stress (i.e., criticality) in a power system. This technique was based on the establishment of a calibrated scale of reference cases and on the use of correlated sampling in a Monte-Carlo simulation. In [12], Dobson *et al.* proposed an analytically tractable model, termed CASCADE, to study the load-dependent cascading failures. The results obtained from the CASCADE model showed that the saturating quasibinomial distribution of the number of failed components had a power-law region at a critical loading and a significant probability of total failure at higher loading. As an aggregation of the above works, Nedic *et al.* [26] further verified and examined the criticality in a 1000-bus network with an AC power flow model that represents many of the interactions that occur in cascading failures. It was found that at the critical loading there was a sharp rise in the mean blackout size. A power-law probability distribution of blackout size was also observed, which indicates a significant risk of large blackouts. In [27], Rahnamay-Naeini and Hayat conducted sensitivity analysis of power grids to cascading failures and showed the critical dependence of cascading failures (i.e., blackout-size distributions with power-law tails) on the operating characteristics, including the loading level, load-shedding constraints and the line-tripping threshold.

## SECTION III. Impact of Human Factors on Cascading Failures

Generally, large-scale blackouts result from the cascading effect of component failures triggered by initial disturbances such as hurricanes, earthquakes, operational faults, sabotage occurrences, and physical attacks such as weapons of mass destruction. The term cascading failures refers to the successive inter-dependent outages of the components of an electric-power system in a short duration of time due to a combination of initial failures and lack of timely corrective actions. It has been known that the number of successive failures when cascading failures occur increases exponentially in time [28], which may prevent the implementation of corrective actions in a timely fashion.

For a better illustration of how human factors (e.g., operators' response to events, power-system control/monitor software, etc.) can impact cascading failures, we provide two narratives extracted from historical data as the evidence. The first narrative is the 2003 Northeast blackout, which is summarized from the blackout reports [1]. Our second narrative is about the 2011 Southwest blackout, which is caused by a network operator's error in the power-distribution layer. *The 2003 Northeast Blackout*: The Northeast blackout of 2003 was a widespread power outage that occurred throughout parts of the Northeastern and Midwestern United States and the Canadian province of Ontario on Thursday, August 14, 2003. The outage affected more than 50 million people.

The event started from the mistake by a control room operator, who forgot to restart the inoperative power flow monitoring tool at 12:15 pm after he corrected the telemetry problem of the state estimator. At 1:31 pm, the Eastlake generating plant, owned by FirstEnergy (FE), shut down. At 2:02 pm, the first of several 345-kV overhead transmission lines in northeast Ohio failed due to contact with a tree. In the meantime, an alarm system failed at FE's control room and was not repaired. As a result, control room operators were not able to recognize or understand the deteriorating condition of the power grid in time. To make matters worse, the lack of alarms affected control room operators' judgment and misled them. For example, the control room operators took no action later to the voltage dips in the grid, failed to inform system controllers, and even dismissed a call from American Electric Power about the tripping of a 345-kV shared transmission line in northeast Ohio. Due to the various human-related errors described above, there was no correct response to the initial few contingencies that occurred in the power grid. As a result, a large cascading failure occurred after 3 pm and progressed rapidly. By 4 pm, five 345-kV transmission lines and sixteen 138-kV transmission lines were tripped offline due to overload (e.g., under voltage and over current).

After 4:05 pm, the cascading failure accelerated and spread to the whole northeastern grid within five minutes, in which more transmission lines were tripped. At this time, operators in different areas realized the blackout and executed grid separations to divide the whole northeastern grid into isolated sub-grids for protection. Finally at 4:13 pm, the outage ended with 256 power plants off-line, where 85% of the power plants went offline after the grid separations occurred, most due to the action of automatic protective controls. The 2003 Northeast blackout clearly indicated that human error can be the cause of severe cascading failures.

*The 2011 Arizona–Southern-California Outages*: On the afternoon of September 8, 2011, an 11-minute system disturbance occurred in the Pacific Southwest, leading to cascading outages and leaving approximately 7 million people without power.

A single 500-kV transmission line initiated the event, but it was not the sole cause; the system was designed to operate in an N-1 state. In this situation, the redistribution of this line's power created voltage deviations and overloads, which had a ripple effect as transformers, transmission lines, and generating units tripped offline. During the 11 minutes of the event, the Western Electricity Coordinating Council (WECC) reliability coordinator issued no directives and only limited mitigating actions were taken by the transmission operators of the affected areas. As a result of the cascading outages stemming from this event, customers in the SDG&E, IID, APS, western area power administration-lower Colorado, and CFE territories lost power, some for multiple hours extending into the next day. It took almost 12 hours for all the affected entities to restore power. Analysis of this blackout showed that the system was not being operated in a secure N-1 state. This failure stemmed primarily from weaknesses in two broad areas: operations planning and real-time situational awareness. If these were done properly it would have allowed system operators to proactively operate the system in a secure N-1 state during normal system conditions and to restore the system to a secure N-1 state as soon as possible, but no longer than 30 minutes. Without adequate planning and situational awareness, entities responsible for operating and overseeing the transmission system could not ensure reliable operations within system operating limits or prevent cascading outages in the event of a single contingency.

It is clear from the two narratives that human factors can highly influence the cascading failure in power grids. Next, we proceed to utilize the SPAR-H methodology to estimate the HEP for the human failure events in probabilistic risk assessment. HEP is the conditional probability of human error given the performance context. The context is represented by a set of variables, the PSFs, which is shown in Table I. Each variable plays a role in the way that the operators respond to an unpredictable event. The final probability of error can be calculated by the following formulas [7]:

a) for number of PSFs < 3

$$\text{HEP} = \text{NHEP} \cdot \prod_{i=1}^2 \text{PSF}_i,$$

(1)

b) and for number of PSFs  $\geq 3$

$$\text{HEP} = \frac{\text{NHEP} \cdot \prod_{i=1}^8 \text{PSF}_i}{\text{NHEP} \cdot \prod_{i=1}^8 \text{PSF}_i + 1}.$$

(2)

The term NHEP is short for nominal human error probability, which is dependent on whether the current scenario is diagnosis (0.01) or action (0.001). It is worth noting that there could be more than one power-system operator handling the failure events occurred during cascading failures. For simplicity, the associated multiplier of the PSFs in Table I are assumed to represent the aggregate effect of multiple operators when calculating the HEP.





**TABLE I** Performance-Shaping Factors and Their Multipliers (Table Is Adopted From [19])

SPAR-H PSFs	SPAR-H PSF levels	Multiplier
NHEP: Diagnosis / Action		0.01 / 0.001
Available time	Inadequate time	Pf= 1
	Minimum required time	10
	Nominal time	1
	Extra time	0.1
	Expansive time	0.01
Stress/Stressors	Extreme	5
	High	2
	Nominal	1
Complexity	Highly complex	5
	Moderately complex	2
	Nominal	1
Experience/training	Obvious diagnosis	0.1
	Low	10
	Nominal	1
	High	0.5
Procedures	Not available	50
	Incomplete	20
	Available, but poor	5
	Nominal	1
	Diagnostic	0.5
Ergonomics/HMI	Missing / misleading	50
	Poor	10
	Nominal	1
Fitness for duty	Good	0.5
	Unfit	Pf=1
	Degraded fitness	5
Work processes	Nominal	1
	Poor	2
	Good	0.8

The term “Pf” stands for probability of failure.)

To this end, the probability of human error in any scenario (e.g., during cascading failures) can be quantified. This will, in turn, be utilized in developing our analytic probabilistic cascading-failure model proposed in the next section.

## SECTION IV. Analytic Framework

### A. Three Phases of Cascading Failures

Observed from historical blackout data (e.g., the two narratives given in Section III), a cascading failure can be typically divided into three phases: the *precursor phase* (phase-1), the *escalation phase* (phase-2) and the *fade-away phase* (phase-3). In the beginning of a cascading failure, there is a small number of initial and subsequent events such as transmission-line failures in the power grid. This stage is termed the precursor phase. As the cascading failure spreads in the power grid, the number of

transmission-line failures increases rapidly, which gives rise to the escalation phase. When a large number of transmission lines have failed, the power grid is divided into islands and the cascading failure starts to phase out. This stage is termed the fade-away phase.

For ease of understanding, we show the time evolution of the cascading failure in the 2003 Northeast US blackout as well as the associated three cascading phases in Fig. 1.

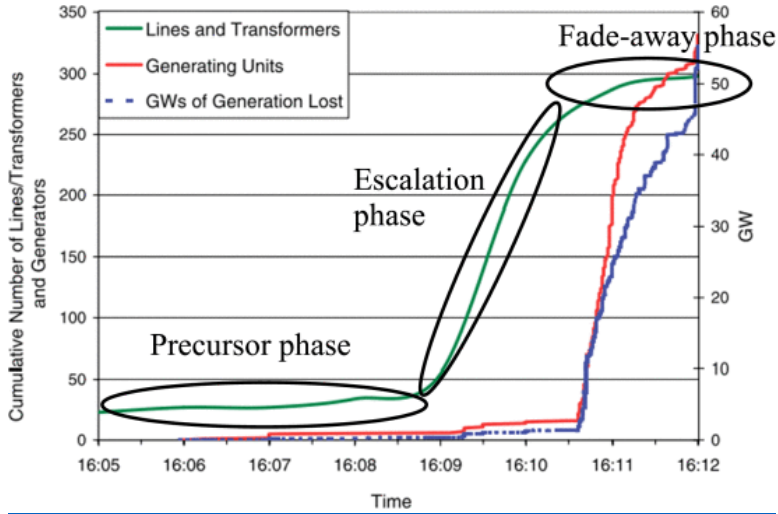


**Fig. 1.** Time evolution and the associated three phases of the cascading failure in 2003 Northeast US blackout. (Figure is adopted from [28].)

## B. hSASE Cascading-Failure Model

Developing an analytic model for cascading failures in the power grid is highly challenging. This is due to the fact that there is a large number of physical attributes of the power grid such as power generation, substation loads, power-flow distribution through transmission lines, functionality of components, voltage and phase of transmission lines and buses, etc., which collectively contribute to a cascading failure. Therefore, keeping track of all the details in the analytic model will result in severe scalability issues.

To address such scalability challenge, we have previously developed a methodology [15], termed abstract state space. To describe it briefly, the space of all detailed power-grid states is partitioned into a collection of equivalence classes. The detailed power-grid states in the same class are represented by the Cartesian product of a few aggregate state-variables with the same values. Such coarse partitioning of the state space of the power grid implies that detailed power-grid states in the same class will be indistinguishable as far as the reduced abstraction is concerned. To this end, each class of the power-grid states is termed an abstract state.

In this paper, we further extend the abstract state space and use three state variables to represent an abstract state of the power grid with the consideration of operator's response (OR). More precisely, a 3-tuple  $(F_i, H_i, I_i)$  is used to represent an abstract state (or in short a state)  $S_i$  of the power grid during a cascading failure (i.e.,  $S_i = (F_i, H_i, I_i)$ ): the state variable  $F_i$  denotes the failed number of

transmission lines, and the state variable  $H_i$ , termed the level of OR, specifies the status of human operators facing power-system situation at state  $S_i$ .

As in [15], we term the state  $S_i$  with  $I_i = 0$  and  $I_i = 1$  as *transitory* and *absorbing* states, respectively. If the power grid is in a transitory state, then the cascading failure will keep proceeding. On the other hand, the cascading failure terminates if the power grid is currently in an absorbing state. Furthermore, we assume that the transition probability from a state  $S_i$  to other states is fully determined by  $S_i$  (or specifically  $F_i$ ,  $H_i$  and  $I_i$ ). Hence, a cascading-failure process in a power grid can be modeled as a Markov chain. The analytic model presented in this paper is then termed the human-factor-coupled stochastic abstract-state evolution (hSASE) model, which is a generalization to the SASE model developed in [15].

**TABLE II** Four Operators' Response Levels and The Associated Two PSFs During A Cascading Failure In IEEE 118-Bus System

Operators' Response	Definition	Available time (respond to contingencies)	Stress (of operators)
Level 1	$F \leq 5$ and $C^{\max} \leq 80\text{MW}$	Extra time	Nominal
Level 2	$5 < F \leq 10$ or $80\text{MW} < C^{\max} < 500\text{MW}$	Nominal time	High
Level 3	$10 < F \leq 50$ or $C^{\max} \geq 500\text{MW}$	Minimum required time	Extreme
Level 4	$F > 50$	Inadequate time	NIA

Similarly to most of the existing cascading-failure models, transmission-line restoration is not considered in the hSASE model. This is due to the fact that power-system operators typically would not restore the failed (or tripped) transmission lines during cascading-failure events. Furthermore, as in [15], we assume that time is divided into small time slots such that only one failure can occur in each time slot. To this end, two types of state transitions, which are triggered by transmission-line failures, will be considered. The first type is called *cascade-stop* transition, where a transitory state  $S_i$  transitions to an absorbing state  $S_j$  such that  $F_j = F_i$  and  $H_j = H_i$ . Note that there will be no more transitions if the system enters an absorbing state. The cascade-stop transition leads to an end of a cascading-failure process. The second type of transitions is a *cascade-continue* transition, where a transitory state  $S_i$  transitions to another transitory state  $S_j$  with the proviso that  $F_j = F_i + 1$  and  $H_j \geq H_i$ . Now the new transitory state  $S_j$  may transition to an absorbing state or to another transitory state, and so on. Note that the cascade-continue transitions are assumed to be caused by single failures; hence,  $S_j$  always has one more failure than the preceding transitory state  $S_i$ , i.e.,  $F_j = F_i + 1$ . It is also natural to assume that a state  $S_i$  with  $F_i = L$ , where  $L$  is the total number of transmission lines in the power grid, is an absorbing state. The cascade-stop and cascade-continue transitions considered in the hSASE model are similar to those in the SASE model [15]; however, the impacts of human error on cascading failures are not considered in the SASE model, i.e., operators are assumed to respond perfectly to any contingency occurred in the power grid.

As the cascade progresses and failures accumulate in the power grid, the level of OR also changes. The coupling between the level of OR and state of the power grid can be explained as follows. Initially when cascading failures start in the power grid, the level of OR reflects less stress and more time for the operators to react to the situation. However, as the failures accumulate (especially the failures of

critical transmission lines with large power-flow capacities), the state of the power grid will impose a higher stress and less time to react. Finally, when the cascade starts to phase out the level of OR will reflect less stress (as the event has already happened) and more time to react. As discussed above, the state of the power grid specifies the level of OR. On the other hand, the level of OR specifies the performance of human operators, which will affect the state of the power grid. Specifically in the first two cascading phases the impact of the operators' performance on cascading failure will be more significant compared to the third (namely the last) cascading phase.

In the remainder of this subsection, we use the IEEE 118-bus system as an example to illustrate the connection between the levels of OR and the three phases of cascading failures. In the IEEE 118-bus system, there are 186 transmission lines in total. We further assume that there are five possible power-flow capacities (e.g., 20 MW, 80 MW, 200 MW, 500 MW and 800 MW representing the quantized power flow capacities based on line properties) associated with the 186 transmission lines. It is noted that these specific capacity values are estimated, since the necessary information for determining the capacities of transmission lines, such as physical properties of the line (e.g., length) and thermal characteristics, are not available publicly. To choose the five capacity values, we have calculated the power flow through the lines using the default setting under normal operating condition given by MATPOWER [29]. After identifying the power flows under the default setting, we quantized them into five capacity classes to ensure the tractability of the analytic framework while keeping the size of the state space to a minimum.

Now let  $H$  be the set containing all the levels of OR in the hSASE model. We assume four levels of OR to capture the state of human operators' performance factors during cascading failures in the IEEE 118-bus system. In brief, a higher level of OR implies a higher risk for any of the PSFs (e.g., the available time for power-system operators to respond to contingencies becomes inadequate and stress of operators increases as the level of OR goes up). For simplicity, in this preliminary study we only consider two important PSFs listed in Table I: the available time for operators to respond to contingencies and the stress of operators.

For the ease of understanding, the four levels of OR are further described next in more detail. We use  $F$  and  $C^{\max}$  to represent the number of failed transmission lines and the maximum (power-flow) capacity of the failed lines in the corresponding levels.

*Level 1:* When  $F \leq 5$  and  $C^{\max} \leq 80$  MW, we say that the OR is at level 1. In this stage, the power grid is in the precursor phase and there are a few initial failures. The operators have more than adequate time to respond to the contingencies (e.g., between 1 and 2 times the nominal time) and operators' stress is nominal. Accordingly, the PSFs 'Available time' and 'Stress' are with levels 'Extra/Expansive time' and 'Nominal,' respectively, as shown in Table I.

*Level 2:* When  $5 < F \leq 10$  or  $80 \text{ MW} < C^{\max} < 500$  MW, we say that the OR is at level 2. In this stage, the power grid is in the advanced precursor cascading phase and additional failures have occurred, either due to the propagation of the initial failures or due to a large initial impact from physical attacks such as deliberate attacks or natural disasters. The operator knows that there is a risk for a cascading failure due to the disaster caused by large initial failures; however, there is still sufficient time to respond to the contingencies yet the stress at this stage is higher than that for Level 1. Accordingly, the

PSFs 'Available time' and 'Stress' are with levels 'Nominal time' and 'Nominal,' respectively, as shown in Table I.

*Level 3:* When  $10 < F \leq 50$  or  $C^{\max} \geq 500$  MW, we say that the OR is at level 3. At this stage, cascading failures are progressing rapidly in the power grid. The available time for operators to respond to contingencies is the minimum required time; thus, the operators' stress is extremely high. Accordingly, the PSFs 'Available time' and 'Stress' are with levels 'Minimum required time' and 'Extreme,' respectively, as shown in Table I.

*Level 4:* We declare this level when  $F > 50$  in the IEEE 118-bus system. At this stage, cascading failures phase out in the power grid and operators' performance cannot alter the state of failures since a large blackouts has already occurred. Hence, the PSF 'Available time' is at the level of 'Inadequate time' as shown in Table I and there is no need to take the operators' stress into account.

For convenience, we have listed the definitions of the four OR levels in Table II. It is worth noting that the level of OR associated to a state  $S_i$  (namely  $H_i$ ) is determined by  $F_i$  and  $C_i^{\max}$ , where  $C_i^{\max}$  is the maximum capacity of failed transmission lines at  $S_i$ . This implies that a state  $S_i$  in the hSASE model is implicitly determined by  $F_i$ ,  $I_i$  and  $C_i^{\max}$ . Hence, the transition of states is achieved by tracking the accumulation of the failed transmission lines as well as the increment of the maximum capacity of the failed transmission lines in the power grid. The detailed modeling of transition probabilities is provided in the next subsection.

### C. Transition Probabilities in the Markov Chain

In this section, we model the transition probabilities from a state  $S_i$  to other states  $S_j$ . It is trivial that if  $S_i$  is an absorbing state, then

$$P(S_j|S_i) = \begin{cases} 1 & \text{if } i = j, \\ 0 & \text{if } i \neq j. \end{cases}$$

(3)

For a transitory state  $S_i$ , the transition probabilities  $P(S_j|S_i)$  are summarized as follows.

For  $F_i \leq 10$ ,  $S_i \neq (5,1,0)$  and  $S_i \neq (10,2,0)$ ,

$$P(S_j|S_i) = \begin{cases} (i)P_{stop}(F_i)g(H_i) & \text{if } I_j = 1, \\ (ii)0 & \text{if } I_j = 0 \text{ and } H_j < H_i, \\ (iii)(1 - P_{stop}(F_i)g(H_i)) \frac{\sum_{C_i=1}^{H_i} L_{C_i} - F_i}{L - F_i} & \text{if } I_j = 0 \text{ and } \\ & H_j = H_i, \\ (iv)(1 - P_{stop}(F_i)g(H_i)) \frac{L_{C_j}}{L - F_i} & \text{if } I_j = 0 \text{ and } \\ & H_i < H_j \leq 3. \end{cases}$$

(4)

When  $S_i = (5,1,0)$ ,

$$P(S_j|S_i) = \begin{cases} (i) P_{stop}(F_i)g(H_i) & \text{if } I_j = 1, \\ (ii) 0 & \text{if } I_j = 0 \text{ and } H_j \leq H_i = 1, \\ (v) (1 - P_{stop}(F_i)g(H_i)) \frac{\sum_{C_i=1}^{H_j} L_{C_i} - F_i}{L - F_i} & \text{if } I_j = 0 \text{ and} \\ & H_j = H_i + 1 = 2, \\ (iv) (1 - P_{stop}(F_i)g(H_i)) \frac{L_{C_j}}{L - F_i} & \text{if } I_j = 0 \text{ and} \\ & H_i + 1 < H_j \leq 3. \end{cases}$$

(5)

When  $S_i = (10,2,0)$ ,

$$P(S_j|S_i) = \begin{cases} (i) P_{stop}(F_i)g(H_i) & \text{if } I_j = 1, \\ (ii) 0 & \text{if } I_j = 0 \text{ and } H_j \leq H_i = 2, \\ (v) (1 - P_{stop}(F_i)g(H_i)) \frac{\sum_{C_i=1}^{H_j} L_{C_i} - F_i}{L - F_i} & \text{if } I_j = 0 \text{ and} \\ & H_j = H_i + 1 = 3. \end{cases}$$

(6)

and when  $F_i > 10$ ,

$$P(S_j|S_i) = \begin{cases} (i) P_{stop}(F_i)g(H_i) & \text{if } I_j = 1, \\ (vi) 1 - P_{stop}(F_i)g(H_i) & \text{if } I_j = 0. \end{cases}$$

(7)

We have considered four scenarios (or groups of states) in the power grid represented by (4)-(7). All the possible state transitions are further categorized into six cases (labeled by cases (i), (ii), (iii), (iv), (v) and (vi), respectively), where the expression of the transition probability for each case is the same for all the scenarios. Note that (5), (6) and (7) represent the transition probabilities for a specific  $S_i$ , while (4) is the general expression used for the rest of the  $S_i$ . Detailed explanation of the six cases of transitions are given below.

- Case (i) represents a transition from a transitory state  $S_i$  to an absorbing state  $S_j$ . The term  $P_{stop}(F_i)$  is the cascade-stop probability obtained based on the power-system simulations. We emphasize here that such cascade-stop probability is obtained without the consideration of human error in the simulator. More specifically, we assume that the operators are always performing the correct response to the contingencies. The function  $g$  captures the impact of operators' performance, namely human error, on the cascading failure. The range of the

function  $g$  is  $[0,1]$ . Since we utilize two PSFs in the model, the HEP of a state  $S_i$  is then calculated by (1) as discussed in Section III. It is noted that as HEP increases, the function  $g$  reduces the probability of transiting to an absorbing state. The detailed definition and characterization of function  $g$  is presented in Section IV-D.

- Case (ii) represents the transition from a transitory state  $S_i$  to a transitory state  $S_j$  with  $H_j$  less than  $H_i$ . The transition probability equals zero for cases (ii), because these transitions cannot occur. More specifically, the maximum capacity of failed transmission lines cannot decrease during a cascading failure.
- Cases (iii) and (iv) represent the general cascade-continue transitions from a transitory state  $S_i$  to another transitory state  $S_j$ . Here  $L_{C_i}$  is the number of transmission lines whose capacity are specified by the  $i$ th level of OR. For example in the IEEE 118-bus system,  $L_{C_1}$  is the number of transmission lines that have capacity less than or equal to 80 MW (namely OR = 1);  $L_{C_2}$  is the number of transmission lines that have capacity larger than 80 MW but less than 500 MW (namely OR = 2); and  $L_{C_3}$  is the number of transmission lines that have capacity larger than or equal to 500 MW (namely OR = 3). Note that  $L = \sum_{C_i=1}^3 L_{C_i} = 186$  is total number of transmission lines in the power grid. The two transition probabilities for cases (iii) and (iv) are formulated based on an assumption that the next transmission line to be failed during the cascading failure is randomly selected from the rest of the functional transmission lines in the power grid. It is worth noting that  $H_i$  and  $H_j$  are less than or equal to three in cases (iii) and (iv) for the example studied here.
- Case (v) represents the same transition as case (iii); however, there is one more transmission-line failure whose capacity is less than or equal to the values specified by the  $i$ th level of OR. According to the definitions of the OR levels regarding  $F$ , however, when  $S_i = (5,1,0)$  and  $S_j = (10,2,0)$  such a transition will cause a rise in the level of OR (i.e.,  $H_i + 1$ ) while  $H_j = H_i$  in case (iii). Note that the difference between the expressions in (iii) and (v) is the upper limit of the summation, i.e.,  $H_i$  in case (iii) and  $H_j$  in case (v).
- Case (vi) represents the cascade-continue transitions for states  $S_i$  with  $F_i > 10$ . From Table II, it is noted that the level of OR of the state  $S_i$  with  $F_i > 10$  is either at 3 or 4. In this case, the rise of the level of OR from 3 to 4 only depends on the number of failures (i.e., from  $F_i > 50$  to  $F_j = 51$ ), and the level of OR stays at 4 (namely the highest level) for states  $S_i$  with  $F_i > 50$ . Hence, the probability of transition from  $S_i$  with  $F_i > 10$  to  $S_j$  with one more failure is always equals to one minus the probability that the cascading failure terminates at  $S_i$ , i.e.,  $P_{\text{stop}}(F_i)g(H_i)$ .

#### D. Impact of Human Error on the Progression of Cascading Failures

In this section, we characterize the function  $g$  introduced in the transition probabilities in the previous subsection. The function  $g$  allows us to capture the impact of operators' response on the progression of cascading failures. This step will allow us to close the loop between the human factors and the dynamics of cascading failures in the power grid.



Naturally, as the HEP increases the probability of further failures in the system also increases because of erroneous decisions and actions. This implies that the probability of termination of the cascading failure decreases as the likelihood of human error increases. To capture these effects, we define

$$g(H_i) = 1 - b\text{HEP}(H_i)$$

(8)

to multiplicatively adjust  $P_{\text{stop}}(F_i)$  based on the HEP. In this formulation,  $b$  is the free parameter for adjusting the strength of the human-error impacts. In particular,  $g(H_i)$  will be multiplied by  $P_{\text{stop}}(F_i)$  to determine the probability that the cascading failure terminates at state  $S_i$  (i.e., the term  $P_{\text{stop}}(F_i)g(H_i)$  in (4)–(7)). Since  $g(H_i)$  has a value in  $[0,1]$ , it will reduce  $P_{\text{stop}}(F_i)$ .

In (8), if  $b$  is a constant (independent of  $H_i$ ) then it is implied that the strength of the human-error impacts on failures does not directly depend on the phases of the cascading failure. However, the human error and decisions can have various degrees of impacts on the progression of failures depending on the state of the power system. For instance, the impact of erroneous decisions and actions by the operators are particularly severe on the likelihood of further failures during the precursor phase. As such, we consider larger values of  $b$  for this phase. On the other hand, we consider smaller values for  $b$  when cascading failures have already occurred and blackouts have affected large areas. This is because the role of human errors on further possible failures are less significant. In the final stage of cascading failures, we consider  $b = 0$  (i.e.,  $g(H_i) = 1$ ) since operators' performance cannot alter the state of cascading failures in this stage as discussed earlier. In general, in this formulation the larger values of  $b$  represent more severe impacts of human errors on cascading failures. Specifically, based on these assumptions we consider  $b$  values as 10, 2.5, 1.5 and 0 for the four levels of OR, respectively.

### E. Modeling $P_{\text{stop}}$ Using Three Operating Characteristics

As discussed in the previous sections,  $P_{\text{stop}}(F_i)$  is one of the key elements of the transition probabilities in the hSASE model, which also needs to be characterized. In our earlier work [15], we have conducted extensive power-system cascading-failure simulations based on MATPOWER for investigating the behavior of  $P_{\text{stop}}(F_i)$ . In particular, we have observed from cascading-failure simulation results that  $P_{\text{stop}}(F_i)$  is strongly affected by the following three intrinsic power-grid operating characteristics.

1. Power-grid loading level: We denote the power-grid loading level by  $r$ , defined as the ratio of the total demand to the generation-capacity of the power grid. The parameter  $r$  represents the level of stress over the grid in terms of the loading level of its components.
2. Line tripping threshold: We consider a threshold,  $\alpha_k$ , for the power flow through the  $k$ th line above which the protection relay trips the line. Various factors and mechanisms in the power grid may affect the threshold  $\alpha_k$  for transmission lines. These include, for example, the environmental conditions, failures in adjacent lines, and smaller measured impedance than relay settings due to overload [30]. We represent the difference between the nominal capacity of a line  $C_k^{\text{opt}}$  and  $\alpha_k$  by a parameter  $e$  as  $C_k^{\text{opt}} - \alpha_k = eC_k^{\text{opt}}$ . The parameter  $e$  captures the effects of various factors and mechanisms that may lead to failure of transmission lines when their power flow is within a certain range of the maximum (nominal) capacity.

- Load-shedding constraint level: Constraints in implementing load shedding are generally governed by control and marketing policies, regulations, physical constraints and communication limitations. The ratio of the uncontrollable loads (loads that do not participate in load shedding) to the total load in the power grid is termed the load-shedding constraint, denoted by  $\theta$ . In extreme cases,  $\theta = 1$  means load shedding cannot be implemented, and  $\theta = 0$  means there is no constraint in implementing the load shedding.

The theoretical ranges of all the three operating characteristics can be from zero to one, i.e.,  $r, e, \theta \in [0,1]$ . As the value of any of the three operating characteristics increases, the power grid becomes more vulnerable to cascading failures. Fig. 2 shows the simulation results of  $P_{\text{stop}}(F_i)$  for the IEEE 118-bus system, which depicts the dependency of cascade-stop probability on  $F_i$  and the load-shedding constraint level of the power grid,  $\theta$ . Following our earlier work [27], the formula of  $P_{\text{stop}}(F_i)$  is given by

$$P_{\text{stop}}(F_i) = \begin{cases} a_1 \left( \frac{a_2 L - F_i}{a_2 L} \right)^4 + \epsilon & 1 \leq F_i \leq a_2 L \\ \epsilon & a_2 L < F_i \leq 0.6L \\ Q(F_i) & 0.6L < F_i \leq L, \end{cases} \quad (9)$$

where  $Q(F_i)$  is a fixed quadratic function approximating the tail of the family of bowl-shape functions as shown in Fig. 2. We also use the obvious terminal condition  $P_{\text{stop}}(L) = 1$ .

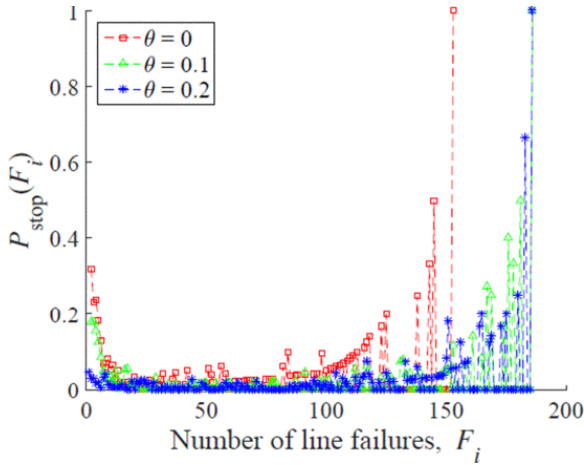


**Fig. 2.** The cascade-stop probability  $P_{\text{stop}}(F_i)$  as estimated from simulation results. (Figure is adopted from [15] .)

In this paper, we further approximate the values of  $a_1$ ,  $a_2$  and  $\epsilon$  as functions of  $r$ ,  $e$  and  $\theta$ . Based on the simulation results (part of the results have been shown in [15] and [27]), a good approximation of  $a_1$ ,  $a_2$  and  $\epsilon$  can be

$$\begin{aligned} a_1 &= 0.4 - 0.25[r]_{0.5} - [e]_{0.1}^{0.5}(0.2 - [e]_{0.1}^{0.5}) - 0.25[\theta]^{0.4}, \\ a_2 &= 0.1 - 0.05[r]_{0.5} - 0.1[e]_{0.1}^{0.5}(0.2 - [e]_{0.1}^{0.5}) - 0.07[\theta]^{0.4}, \\ \epsilon &= 0.6 - 0.4[r]_{0.5} - 0.5[e]_{0.1}^{0.5} - 0.3[\theta]^{0.4}. \end{aligned}$$

(10)(11)(12)

It is noted that the values of  $r$ ,  $e$  and  $\theta$  are truncated in (10), (11) and (12). The reasons are twofold. On one hand, the impact of an operating characteristic on cascading failures (namely  $P_{\text{stop}}(F_i)$ ) behaves similarly beyond certain threshold, e.g.,  $r < 0.5$  and  $e < 0.1$ , based on power-system simulation results. On the other hand, it is practical to assume that  $e$  should be less than 0.3 and  $\theta$  should be less than 0.4. For convenience, we also show the analytic characterizations of  $a_1$  and  $a_2$  as a function of  $r$ ,  $e$  and  $\theta$  in Fig. 3. With the parametric modeling of  $P_{\text{stop}}(F_i)$  at hand, the description of transition probabilities in the hSASE model becomes complete.

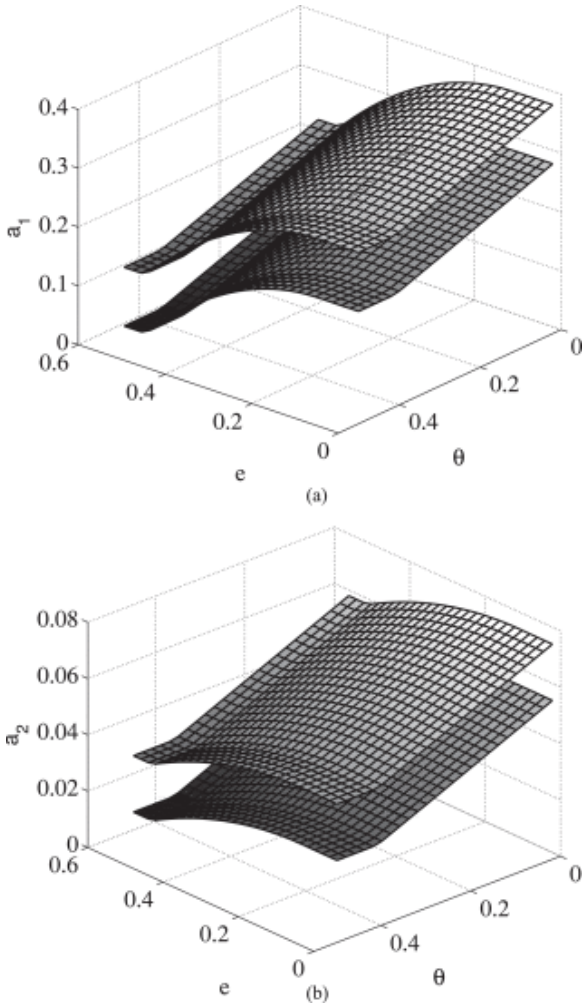


**Fig. 3.** Analytic characterizations of (a)  $a_1$  and (b)  $a_2$  as a function of  $r$ ,  $e$ , and  $\theta$ . Upper surfaces:  $r = 0.5$ ; lower surfaces:  $r = 0.9$ .

## SECTION V. Blackout-Size Probability Distribution

### A. Criticality Analysis Using the hSASE Model

An important consequence of the hSASE model is that it allows us to evaluate the probability mass function (PMF) of the blackout size of a cascading-failure caused by any disturbance event. Such PMF is a widely adopted metric for assessing the risk of cascading failures in the power grid.

Let  $S$  denote the state space of the Markov chain in the hSASE model. The total number of states in  $S$  is  $2L|H|$  due to the definition of a state  $S_i \in S$  given in Section IV-B. Here  $L$  is the number of transmission lines in the power grid and  $|H|$  is the cardinality of  $H$  (recall that  $H$  is the set containing all the levels of OR). Note that  $|H|$  is a fixed number in the hSASE model, e.g.,  $|H| = 4$  for the IEEE 118-bus system studied in this paper. Hence, the size of the state space of the Markov chain scales linearly as a function of the number of transmission lines in the power system.

For convenience, the indices of all the states in the Markov chain are arranged by following three simple rules.

For any two distinct states  $S_i$  and  $S_j$ ,

- i)  $i < j$  if  $F_i < F_j$ ;
- ii)  $i < j$  if  $F_i < F_j$  but  $H_i < H_j$ ;
- iii)  $j = i + 1$  if  $F_i < F_j$  and  $H_i = H_j$ , but  $I_i = 0$  and  $I_j = 1$ .

To this end, the index of a state  $S_i = (F_i, H_i, I_i)$  is

$$(F_i - 1)|H| + 2(H_i - 1) + I_i + 1.$$

(13)

From (13), it is clear that the indices of transitory states and absorbing states are odd and even, respectively. Furthermore, if a transition from  $S_i$  to  $S_j$  has a positive probability, then the index of  $S_j$  is always larger than the index of  $S_i$ .

Now let  $\mathbf{Q}$  be the transition matrix of the Markov chain, and  $q_{ij}$  represent the  $ij$ th element of  $\mathbf{Q}$ , i.e.,  $q_{ij} = P(S_j|S_i)$ . It is clear that  $\mathbf{Q}$  is a  $2L|H| \times 2L|H|$  square matrix. Furthermore, two important properties of  $\mathbf{Q}$  are given by the following two propositions and a lemma.

**Proposition 1:**

$\mathbf{Q}$  is an upper diagonal matrix.

**Proof:**

This is due to the fact that the number of failed transmission lines accumulate during cascading failures and there is no transmission-line restoration during cascading failures in the hSASE model.

**Proposition 2:**

The elements on the main diagonal of  $\mathbf{Q}$  are given by

$$q_{ii} = \begin{cases} 0 & \text{if } i \text{ is odd,} \\ 1 & \text{if } i \text{ is even.} \end{cases}$$

**Proof:**

This is due to the definitions of a transitory state and an absorbing state given in Section IV-B. More specifically, the cascading failure proceeds when it is in a transitory state  $S_i$  (when  $i$  is odd), which

implies that  $q_{ii} = 0$ . While the cascading failure terminates when it is in an absorbing state  $S_i$  (when  $i$  is even), which implies that  $q_{ii} = 1$  and  $q_{ij} = 0$  for  $i \neq j$ .

**Lemma 1:**

$Q$  is a stochastic matrix.

**Proof:**

We must show that  $\sum_{j \in S} q_{ij} = 1$ , for all  $i \in S$ . When  $i$  is even, it is clear from Proposition 2 that  $q_{ii} = 1$  and  $q_{ij} = 0$  for  $i \neq j$ , which implies  $\sum_{j \in S} q_{ij} = 1$ . When  $i$  is odd, a state  $S_i = (F_i, H_i, 0)$  is a transitory state. According to the definition of transition probabilities given in (4), the cascade-stop transition from  $S_i$  to  $S_j$  is unique, where  $j = i + 1$ , with  $q_{ij} = P_{\text{stop}}(F_i)g(H_i)$ . On the other hand, there may be multiple cascade-continue transitions from  $S_i$  to  $S_j$  for  $j \in J$ , where  $J$  is the set containing odd numbers in the range  $[i + 2|H|, 2(F_i + 1)|H| - 1]$ . Furthermore,  $\sum_{j \in J} q_{ij} = 1 - P_{\text{stop}}(F_i)g(H_i)$  and  $q_{ij} = 0$  for all  $j \notin J$  and  $j \in S$ . Hence,  $\sum_{j \in S} q_{ij} = 1$  when  $i$  is odd.

**Theorem 1:**

Starting from any initial state  $S_0$ , the state always reaches an absorbing state in the Markov chain given the transition matrix  $Q$ .

**Proof:**

It is noted that a state  $S_i$  is either transitory or absorbing. For a transitory state  $S_i$ , it can only transition to  $S_j$  with  $F_j = F_i + 1$ . Furthermore, if a transitory state  $S_i$  with  $F_i = L - 1$  transition to the next state  $S_j$  then  $S_j$  has  $F_j = L$ . As the terminal condition,  $S_j$  is always an absorbing state. Theorem 1 is then established since only finite number of states will be considered in the hSASE model.

In light of Theorem 1, we can claim that the Markov chain has a limiting distribution of states given an initial state  $S_0$ . Let the vector  $\pi_0 = (0, \dots, 0, 1, 0, \dots, 0)$  denote the initial state  $S_0$ , where the position of the element that equals to "1" in  $\pi_0$  is the index of  $S_0$  in the Markov chain. Next, let the vector  $\pi = (\pi_i, i = 1, \dots, 2L|H|)$  represent the limiting distribution given  $\pi_0$ , where  $\pi_i$  is the steady-state probability of  $S_i$ . Then

$$\pi \triangleq \pi_0 \lim_{k \rightarrow \infty} Q^k.$$

(14)

Now let  $B(n|S_0)$  represent the summation of the steady-state probabilities of a set of states  $S_i$  with  $F_i = n$ . We can write

$$B(n|S_0) = \sum_{i=1}^{|H|} \pi_{2(n-1)|H|+2i}, \text{ for } n = 1, \dots, L.$$

(15)

It is important to note that  $B(n|S_0)$  represents the probability of a blackout with  $n$  transmission-line failures given an initial disturbance  $S_0$  in the physical sense.

It is noted that the Markov chain studied in the hSASE model is not irreducible because there exist both transient states and recurrent states in the Markov chain. This further implies that the unique stationary distribution of the Markov chain does not exist (it is not difficult to see this point since the stationary distribution is dependent on the initial state). To obtain the PMF of the blackout size (i.e.,  $B(n|S_0)$  for  $n = 1, \dots, L$ ), we can conduct Monte-Carlo simulations of the Markov chain given the initial state  $S_0$ . In this case, the computational complexity of the hSASE model scales linearly in terms of  $L$ . Alternatively, we can further obtain the analytic expression for  $B(n|S_0)$  by evaluating  $\lim_{k \rightarrow \infty} \mathbf{Q}^k$ . This can be done by performing matrix diagonalization as well as using the Cayley-Hamilton theorem. For further discussion on the details of this analysis, we refer interested readers to [15].

## B. Critical Operating Characteristics of the Power Grid

From the analysis of historical blackout data of the North American electric power transmission system [10], [24], [31] as well as power-system simulation results [15], [26], [27], researchers have agreed that today's power grids may be operated close to a critical setting. A widely accepted indicator of such critical setting is that the PMF of the blackout sizes does not decrease exponentially with the size of the blackout, but rather a power-law tail [32]. Hence, in this paper we define a power grid to be operating in a critical setting if the PMF of the blackout size has a power-law tail.

Given the operating characteristics of the power grid as well as the initial disturbance event  $S_0$ , we are able to obtain the PMF of blackout size of a cascading failure (namely  $B(n|S_0)$ ) by applying the limit approach as discussed in Section V-A. The PMF of blackout size can be used to further characterize the critical operating characteristics of the power grid. In this section, we start by investigating various cascading-failure scenarios and calculate the associated PMFs of blackout size to find out how the human behavior and the three power-grid operating characteristics influence the cascading-failure behavior in the IEEE 118-bus system. Then we proceed to identify the critical operating characteristics of the power grid, which should be avoided to reduce the risk of large cascading failures. The initial disturbance event considered here is two transmission-line failures with  $C^{\max} = 80$  MW.

In Fig. 4 we show the PMFs of blackout size for three different scenarios when  $e = 0.3$  and  $\theta = 0.3$ . First, it is interesting to compare the results for the two scenarios when  $r = 0.75$ . It is clear that the PMF of blackout size changes from an exponential behavior, when the human error is not considered, to a power-law tail when the human error is considered. It is also worth noting that the coupling of human behavior is not the exclusive factor that determines the criticality of the cascading failure. For example in the case when  $r = 0.9$  and the human coupling is not taken into account, the PMF of blackout size also exhibits a power-law tail.

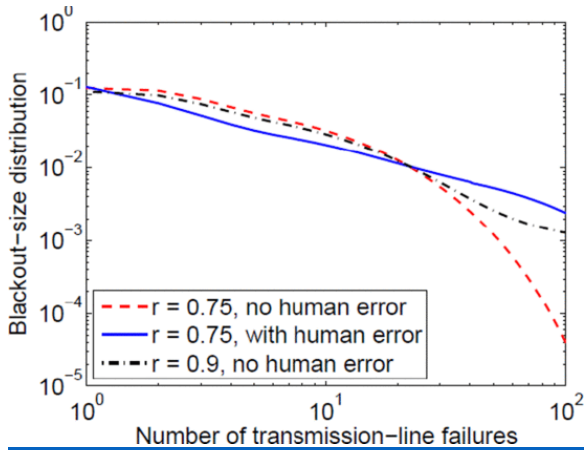


**Fig. 4.** The PMF of blackout size for three different scenarios:  $e = 0.3$  and  $\theta = 0.3$ .

To further investigate how the cascading failure is influenced by the power-grid operating setting and the human behavior, we show another set of PMFs of blackout size in Fig. 5 for cases when  $e = 0.1$ ,  $\theta = 0.01$  and the impact of human behavior has been considered. Under such a setting of  $e$  and  $\theta$ , the power grid is less vulnerable to cascading failures. Hence, we observe from Fig. 5 that, as expected, all the PMFs of the blackout size approximate the exponential behavior no matter what the load ratio  $r$  is.

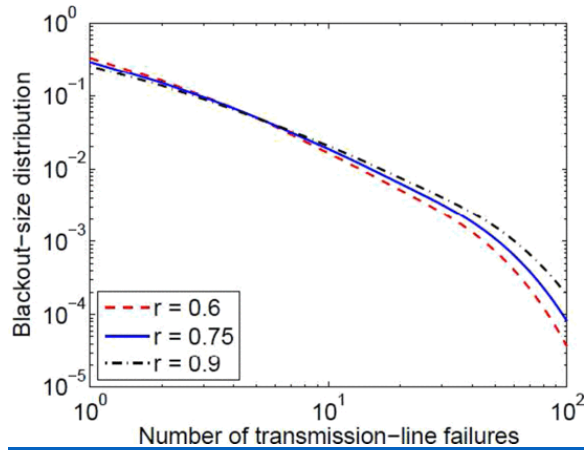


**Fig. 5.** The PMF of blackout size for three different loading level  $r$  when human error is considered for all scenarios:  $e = 0.1$ ,  $\theta = 0.01$ .

The results in Figs. 4 and 5 confirm that there exist certain critical settings (i.e., combinations of values of  $r$ ,  $e$  and  $\theta$ ) that determine the criticality of cascading failure in the power grid. In other words, these critical points make the system sensitive to large cascading failures with the blackout probability following a power-law distribution.

In light of the proposed analytic model, we can further identify the non-critical settings for cascading failures in the power grid without running the power-system simulator, which is time consuming. In Fig. 6, two non-critical regions are shown for cases when the impact of human behavior is not considered and considered, respectively. In particular, each point inside the regions represents a specific operating setting (a combination of  $r$ ,  $e$  and  $\theta$ ). The PMF of the blackout size under any non-

critical operating setting tends to have the exponential-tail behavior rather than the power-law tail. By comparing Fig. 6(a) and (b), it is clear that the non-critical regions shrink due to the consideration of human error. One more important fact learned from Fig. 6 is that the impact of human error can also be illustrated as the drop of  $\theta$  in the non-critical region when  $r$  and  $e$  are fixed. The observation directly implies that the power grid can enhance its tolerance to cascading failures when more load-shedding is allowed.

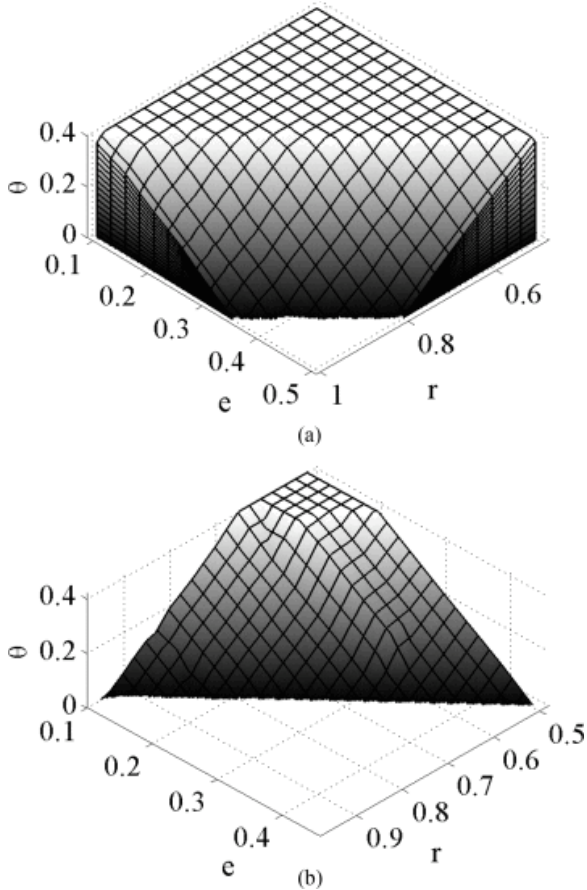


**Fig. 6.** Non-critical region for power-grid operating characteristics when (a) the impact of human behavior is not considered, and (b) the impact of human behavior is considered.

## SECTION VI. Conclusions and Extensions

Human operators play a key role in the reliable operation of power grids. However, human operators may behave far from optimum. The reasons may include stressful situations and other factors that affect the reliability of power grids. Historical blackout data as well as interviews of power-system operators illustrate that human behavior can highly impact cascading failures in power grids. To quantify the human error during cascading failures, the SPAR-H methodology is used to estimate the HEP for the human failure events in terms of probabilistic risk assessment.

With the assessment of HEP at hand, we have developed a scalable analytic model, based upon reduced state-space Markov chains, to investigate the cascading failures in power grids when human behavior is considered. With the help of power-system simulations, we have further formulated the state-dependent transition probabilities in the Markov chain in terms of the HEP as well as three key



power-system operating characteristics including the power-grid loading level, line tripping threshold, and load-shedding constraint level. In light of the proposed analytic model, the criticality of key power-system operating characteristics can be identified. In particular, non-critical regions of the three operating-characteristic settings have been suggested, under which the power grid may become less vulnerable to severe cascading failures (the PMF of blackout size due to cascading failures decreases exponentially rather than having a power-law tail). The results can provide invaluable design and management for power-system robustness as a contribution to operate smart grids as well as a model to analyze the impact of human factors on cascading failures.

As a starting point of this work, we have only focused on the number of transmission-line failures and the loss of transmission capacity. However, the proposed analytic framework is capable of tracking other types of failures and investigating the impact of other physical attributes in the power system, such as generators, on cascading failures. For example, we can extend the definition of the state space (e.g., by introducing a state variable  $G_i$  representing the number of generator failures) of the Markov chain to track other variables in the system. Introducing new state variables (e.g., number of generator failures) also mandates generating supporting simulations to be able to estimate and relate the transition probabilities of the Markov chain to all the state variables.

## References

1. G. Andersson et al., "Causes of the 2003 major grid blackouts in north america and europe and recommended means to improve system dynamic performance", *IEEE Trans. Power Syst.*, vol. 20, no. 4, pp. 1922-1928, Nov. 2005.
2. "Arizona-southern california outages on september 8 2011: Causes and recommendations", Apr. 2012, [online] Available: <https://www.ferc.gov>.
3. P. Pourbeik, P. S. Kundur and C. W. Taylor, "The anatomy of a power grid blackout", *IEEE Power Energy Mag.*, vol. 4, no. 5, pp. 22-29, Sep./Oct. 2006.
4. M. Amin, "Challenges in reliability security efficiency and resilience of energy infrastructure: Toward smart self-healing electric power grid", *Proc. Power Energy Soc. General Meeting-Convers. Delivery Elect. Energy 21st Century*, pp. 1-5, 2008.
5. J. Park et al., "Analysis of operators' performance under emergencies using a training simulator of the nuclear power plant", *Reliab. Eng. Syst. Safety*, vol. 83, no. 2, pp. 179-186, 2004.
6. C. R. Lawton and J. H. Gauthier, "Human performance modeling in system of systems analytics", *Proc. 7th Int. Conf. Syst. Syst. Eng.*, pp. 77-82, 2012.
7. J. M. Abreu et al., "Modeling human reliability in the power grid environment: An application of the spar-h methodology", *Proc. Human Factors Ergonomics Soc. Annu. Meet.*, vol. 59, no. 1, pp. 662-666, 2015.
8. M. Panteli and D. S. Kirschen, "Situation awareness in power systems: Theory challenges and applications", *Electr. Power Syst. Res.*, vol. 122, pp. 140-151, 2015.
9. M. Bessani et al., "Impact of operators performance in the reliability of cyber-physical power distribution systems", *IET Gener. Transmiss. Distrib.*, vol. 10, no. 11, pp. 2640-2646, 2016.
10. B. A. Carreras, V. E. Lynch, I. Dobson and D. E. Newman, "Complex dynamics of blackouts in power transmission systems", *Chaos: An Interdisciplinary J. Nonlinear Sci.*, vol. 14, no. 3, pp. 643-652, 2004.

11. J. Chen, J. S. Thorp and I. Dobson, "Cascading dynamics and mitigation assessment in power system disturbances via a hidden failure model", *Int. J. Electr. Power Energy Syst.*, vol. 27, no. 4, pp. 318-326, 2005.
12. I. Dobson, B. A. Carreras and D. E. Newman, "A loading-dependent model of probabilistic cascading failure", *Probab. Eng. Information Sci.*, vol. 19, no. 1, pp. 15-32, 2005.
13. M. Anghel, K. A. Werley and A. E. Motter, "Stochastic model for power grid dynamics", *Proc. 40th Annu. Hawaii Int. Conf. Syst. Sci.*, pp. 113-113, 2007.
14. M. Rahnamay-Naeini, Z. Wang, A. Mammoli and M. M. Hayat, "A probabilistic model for the dynamics of cascading failures and blackouts in power grids", *Proc. Power Energy Soc. General Meeting*, pp. 1859-1864, 2012.
15. M. Rahnamay-Naeini, Z. Wang, N. Ghani, A. Mammoli and M. M. Hayat, "Stochastic analysis of cascading-failure dynamics in power grids", *IEEE Trans. Power Syst.*, vol. 29, no. 4, pp. 1767-1779, Jul. 2014.
16. J. Song, E. Cotilla-Sanchez, G. Ghanavati and P. D. Hines, "Dynamic modeling of cascading failure in power systems", *IEEE Trans. Power Syst.*, vol. 31, no. 3, pp. 2085-2095, May 2016.
17. J. Bialek et al., "Benchmarking and validation of cascading failure analysis tools", *IEEE Trans. Power Syst.*, vol. 31, no. 6, pp. 4887-4900, Nov. 2016.
18. X. Zhang, C. Zhan and K. T. Chi, "Modeling the dynamics of cascading failures in power systems", *IEEE J. Emerg. Sel. Topics Circuits Syst.*, vol. 7, no. 2, pp. 192-204, Jun. 2017.
19. D. Gertman et al., "The spar-h human reliability analysis method", *US Nuclear Regulatory Commission*, 2005.
20. M. Azadeh, A. Keramati, I. Mohammadfam and B. Jamshidnejad, "Enhancing the availability and reliability of power plants through macroergonomics approach", *J. Sci. Ind. Res.*, vol. 65, no. 11, pp. 873-878, 2006.
21. H. S. Blackman, D. I. Gertman and R. L. Boring, "Human error quantification using performance shaping factors in the spar-h method", *Proc. Human Factors Ergonomics Soc. Annu. Meeting*, vol. 52, no. 21, pp. 1733-1737, 2008.
22. R. L. Boring and H. S. Blackman, "The origins of the spar-h method's performance shaping factor multipliers", *Proc. IEEE 8th Human Factors Power Plants HPRCT 13th Annu. Meeting*, pp. 177-184, 2007.
23. R. Moura, M. Beer, E. Patelli, J. Lewis and F. Knoll, "Learning from major accidents to improve system design", *Safety Sci.*, vol. 84, pp. 37-45, 2016.
24. B. A. Carreras, V. E. Lynch, I. Dobson and D. E. Newman, "Critical points and transitions in an electric power transmission model for cascading failure blackouts", *Chaos: An Interdisciplinary J. Nonlinear Sci.*, vol. 12, no. 4, pp. 985-994, 2002.
25. D. S. Kirschen, D. Jayaweera, D. P. Nedic and R. N. Allan, "A probabilistic indicator of system stress", *IEEE Trans. Power Syst.*, vol. 19, no. 3, pp. 1650-1657, Aug. 2004.
26. D. P. Nedic, I. Dobson, D. S. Kirschen, B. A. Carreras and V. E. Lynch, "Criticality in a cascading failure blackout model", *Int. J. Electr. Power Energy Syst.*, vol. 28, no. 9, pp. 627-633, 2006.
27. M. Rahnamay-Naeini and M. M. Hayat, "Impacts of operating characteristics on sensitivity of power grids to cascading failures", *Proc. Power Energy Soc. General Meeting*, 2016.
28. B. Liscouski and W. Elliot, "Final report on the august 14 2003 blackout in the united states and canada: Causes and recommendations", *Report to US Department of Energy Electricity Delivery*

& Energy Reliability Office of Electricity Delivery & Energy Reliability Washington DC USA, vol. 40, no. 4, 2004.

29. R. D. Zimmerman, C. E. Murillo-Sánchez and R. J. Thomas, "Matpower: Steady-state operations planning and analysis tools for power systems research and education", *IEEE Trans. Power Syst.*, vol. 26, no. 1, pp. 12-19, Feb. 2011.
30. Q. Chen and L. Mili, "Composite power system vulnerability evaluation to cascading failures using importance sampling and antithetic variates", *IEEE Trans. Power Syst.*, vol. 28, no. 3, pp. 2321-2330, Aug. 2013.
31. B. A. Carreras, D. E. Newman, I. Dobson and A. B. Poole, "Evidence for self-organized criticality in a time series of electric power system blackouts", *IEEE Trans. Circuits Syst. I Reg. Papers*, vol. 51, no. 9, pp. 1733-1740, Sep. 2004.
32. I. Dobson, B. A. Carreras, V. E. Lynch and D. E. Newman, "An initial model for complex dynamics in electric power system blackouts", *Proc. 34th Hawaii Int. Conf. Syst. Sci.*, Jan. 2002.